

# Correlated vibration–solvent effects on the non-Condon exciton spectroscopy

Zi-Hao Chen,<sup>1</sup> Yao Wang,<sup>2,\*</sup> Rui-Xue Xu,<sup>1,2,†</sup> and YiJing Yan<sup>1,2</sup>

<sup>1</sup>*Department of Chemical Physics, University of Science and Technology of China, Hefei, Anhui 230026, China*

<sup>2</sup>*Hefei National Laboratory for Physical Sciences at the Microscale and iChEM and Synergetic Innovation Center of Quantum Information and Quantum Physics, University of Science and Technology of China, Hefei, Anhui 230026, China*

(Dated: June 1, 2021)

Excitation energy transfer is crucially involved in a variety of systems. During the process, the non-Condon vibronic coupling and the surrounding solvent interaction may synergetically play important roles. In this work, we study the correlated vibration–solvent influences on the non-Condon exciton spectroscopy. Statistical analysis is elaborated for the overall vibration–plus–solvent environmental effects. Analytic solutions are derived for the linear absorption of monomer systems. General simulations are accurately carried out via the dissipaton–equation–of–motion approach. The resulted spectra in either the linear absorption or strong field regime clearly demonstrate the coherence enhancement due to the synergetic vibration–solvent correlation.

## I. INTRODUCTION

Excitation energy transfer (EET) is crucially involved in a variety of systems including molecular aggregates, organic semiconductors, light harvesting systems, etc.[1–5] Particularly, the long–lived quantum beats in photosynthetic antenna complexes have aroused great interest.[6–9] It is found that the non-Condon vibronic coupling would affect this quantum coherence enhancement.[10–12] Spectroscopic studies on EET systems have been widely carried out to reveal the structures and underlying dynamic processes in these systems.[13–18]

In reality, EET constitutes an open quantum process where intramolecular nuclear vibrations and the surrounding solvent would coordinatively play important roles. To study the non-Condon vibronic coupling, one needs to deal with the hybridization between the excitonic system and nuclear vibrations. By the Herzberg–Teller approximation, vibrations would contribute to the transition dipole moments. While the solvent, coupled to both excitons and vibrations, is considered to be non-polarizable.

Take, for example, a monomer excitonic system. The total Hamiltonian in the presence of external field reads

$$H_T(t) = H_M - \varepsilon(t)\hat{\mu}_T, \quad (1a)$$

where

$$H_M = (\Delta + H'_{\text{env}} - H_{\text{env}})\hat{B}^\dagger\hat{B} + H_{\text{env}}. \quad (1b)$$

Here,  $\hat{B} \equiv |0\rangle\langle 1|$  ( $\hat{B}^\dagger \equiv |1\rangle\langle 0|$ ) is the excitonic annihilation (creation) operators, and  $\Delta$  is the excitation energy. The total electronic–plus–vibrational dipole moment  $\hat{\mu}_T$  interacts with a classical external field  $\varepsilon(t)$ .  $H_{\text{env}}$  and  $H'_{\text{env}}$  are the vibration–plus–solvent environment Hamiltonians, associated with the ground and excited states, respectively. In this work, we adopt the Caldeira–Leggett’s

model,[19–21] i.e.

$$H_{\text{env}} = \frac{\Omega}{2}(\hat{p}^2 + \hat{q}^2) + \sum_k \frac{\omega_k}{2} \left[ \hat{p}_k^2 + \left( \hat{x}_k - \frac{c_k}{\omega_k} \hat{q} \right)^2 \right]. \quad (2)$$

It involves a vibrational mode  $\hat{q}$  and its coupling to a solvent bath,  $h_B = \frac{1}{2} \sum_k \omega_k (\hat{p}_k^2 + \hat{x}_k^2)$ .  $H'_{\text{env}}$  is similar to  $H_{\text{env}}$  of Eq. (2), but with linearly displaced  $q' = q - D$  and  $\{x'_k = x_k - d_k\}$ . This results in an overall reorganization,

$$\lambda \equiv \langle H'_{\text{env}} - H_{\text{env}} \rangle_{\text{env}}. \quad (3)$$

Here,  $\langle \hat{O} \rangle_{\text{env}} \equiv \text{Tr}_{\text{env}}(\hat{O}e^{-\beta H_{\text{env}}})/\text{Tr}_{\text{env}}e^{-\beta H_{\text{env}}}$ . The environment induced force is given by

$$\hat{F} = H'_{\text{env}} - H_{\text{env}} - \lambda. \quad (4)$$

In this work, we are interested in the statistically correlated vibration–and–solvent influences onto the EET systems and the associated non-Condon effect in the Herzberg–Teller approximation. One approach could be inclusion of the vibrational mode into the system, leaving the solvent alone as environment. This will enlarge the dimension of the system, making it difficult to extend to multi-mode cases and polymeric systems. The alternative approach is to treat the intramolecular vibrational mode and the solvent altogether as environment, interacting with the EET system, in a statistical manner. This work starts from this strategy. However, most traditional quantum dissipation theories, for example, the Redfield equation and its modified series,[22–29] focus explicitly only on the reduced system, making them practically intractable to simulate the environment–polarized excitation. The exact hierarchical–equation–of–motion (HEOM) formalism in Gaussian environments,[30–39] constructed via the calculus on path integrals, are composed of coupled differential equations between the primary reduced system density operator and a set of auxiliary operators. These auxiliary operators, although in principle, carry the environmental informations, their associated quantum dynamic algebras make the HEOM formalism not convenient in the extension to study environment polarizations.

\*Electronic address: wy2010@ustc.edu.cn

†Electronic address: rxxu@ustc.edu.cn

The dissipaton equation of motion (DEOM), [40–43] using quasi-particle descriptions for environments, provides a unified treatment on hybridized environment dynamics and entangled system–environment excitations, straightforwardly. Being an exact method for Gaussian environment, the DEOM recovers the HEOM for just the reduced system dynamics. Besides, the DEOM adopts “dissipatons” as quasi-particles associated with the interacting environment statistical dynamics. [40–45] It was applied to study the Herzberg–Teller vibronic coupling in our previous work, [18] but the correlated solvent effects were not considered there.

This work starts from the physical model of total Hamiltonian, Eq. (2), which contains the hybridized exciton–vibration, exciton–solvent, and vibration–solvent couplings. The overall vibration–plus–solvent environment response function, characterizing the environment statistical properties, is briefed in Sec. II, with the derivation detailed in Appendix A. A general DEOM formalism for multi-mode system–environment couplings and the Herzberg–Teller type of dipole moments are constructed in Sec. III. Numerical demonstrations and discussions are presented in Sec. IV. The analytic solution for the linear absorption of the current monomer system, Eq. (2), is derived in Appendix B. The expression and analysis in the gas–phase limit is given in Appendix C. The paper is summarized in Sec. V.

## II. ENVIRONMENT STATISTICS

This section concentrates on the environment statistics. The total system involves the correlated exciton–vibration, exciton–solvent, and vibration–solvent couplings (cf. Sec. II A) where the vibrational mode in solvent behaves as a Brownian oscillator. Following some elementary quantum statistical algebra, the overall vibration–plus–solvent environment statistical properties, basically the response functions, can be obtained (finalized in Sec. II B and detailed in Appendix A).

### A. Vibration–solvent decomposition

According to Eqs. (2) and (3), the overall reorganization energy reads

$$\lambda = \frac{1}{2}\Omega D^2 + \frac{1}{2}\sum_k \omega_k \left( \frac{c_k}{\omega_k} D - d_k \right)^2. \quad (5)$$

The environment induced force, defined in Eq. (4), can be decomposed into two parts as

$$\hat{F} = \hat{F}_1 + \hat{F}_2, \quad (6)$$

where

$$\hat{F}_1 = \left[ \sum_k c_k d_k - \left( \Omega + \sum_k \frac{c_k^2}{\omega_k} \right) D \right] \hat{q}, \quad (7a)$$

$$\hat{F}_2 = D \hat{X}_B - \hat{Y}_B, \quad (7b)$$

with

$$\hat{X}_B = \sum_k c_k \hat{x}_k \quad \text{and} \quad \hat{Y}_B = \sum_k \omega_k d_k \hat{x}_k. \quad (8)$$

Here  $\hat{F}_1$  and  $\hat{F}_2$  associate with the vibrational mode and solvent degrees of freedom, respectively. In this paper the former is considered of optical polarization while the latter not.

It is noticed that the above environment model, Eqs. (2) and (7), constitutes a Gaussian–Wick’s bath. Its influence onto the system and the entangled system–environment dynamics can be totally characterized by the environment correlation functions

$$C_{ab}(t) \equiv \langle \hat{F}_a^{\text{env}}(t) \hat{F}_b^{\text{env}}(0) \rangle_{\text{env}}; \quad a, b = 1, 2. \quad (9)$$

Here, we have denoted

$$\hat{O}^{\text{env}}(t) \equiv e^{iH_{\text{env}}t} \hat{O} e^{-iH_{\text{env}}t}. \quad (10)$$

Throughout this work, we set  $\hbar = 1$  and  $\beta = 1/(k_B T)$ , with  $k_B$  being the Boltzmann constant and  $T$  the temperature. The correlations  $C_{ab}(t)$  can be obtained via the fluctuation–dissipation theorem as [20, 21]

$$C_{ab}(t) = \frac{1}{\pi} \int_{-\infty}^{\infty} d\omega \frac{e^{-i\omega t} J_{ab}(\omega)}{1 - e^{-\beta\omega}}. \quad (11)$$

In Eq. (11),  $J_{ab}(\omega)$  are the interaction spectral densities, reading

$$J_{ab}(\omega) = \frac{1}{2i} \int_{-\infty}^{\infty} dt e^{i\omega t} \Phi_{ab}(t), \quad (12)$$

where  $\Phi_{ab}(t)$  are bath response functions defined as

$$\Phi_{ab}(t) \equiv i \langle [\hat{F}_a^{\text{env}}(t), \hat{F}_b^{\text{env}}(0)] \rangle_{\text{env}}. \quad (13)$$

In the following parts of paper, we denote for any function  $f(t)$  the frequency resolution,

$$\tilde{f}(\omega) \equiv \int_0^{\infty} dt e^{i\omega t} f(t). \quad (14)$$

### B. Environment response functions

To obtain  $J_{ab}(\omega)$ , consider first the vibrational response function in the total environment composite [Eq. (2)]

$$\chi_{qq}(t) \equiv i \langle [\hat{q}^{\text{env}}(t), \hat{q}^{\text{env}}(0)] \rangle_{\text{env}}. \quad (15)$$

Its frequency resolution is identified to be [20, 21]

$$\tilde{\chi}_{qq}(\omega) = \frac{\Omega}{\omega_s^2 - \omega^2 - i\omega\tilde{\zeta}(\omega)}. \quad (16)$$

The solvent induced frictional function,  $\tilde{\zeta}(\omega)$ , is related to the solvent susceptibility function via [21]

$$i\omega\tilde{\zeta}(\omega) = \Omega [\tilde{\varphi}_{xx}(\omega) - \tilde{\varphi}_{xx}(0)]. \quad (17)$$

In Eq. (17), the involving interacting solvent response function is

$$\varphi_{xx}(t) \equiv i\langle[\hat{X}_B^B(t), \hat{X}_B]\rangle_B, \quad (18)$$

with  $\hat{X}_B$  defined in Eq. (8). Here, we denote  $\langle\hat{O}\rangle_B \equiv \text{tr}_B(\hat{O}e^{-\beta h_B})/\text{tr}_B e^{-\beta h_B}$  and  $\hat{O}^B(t) \equiv e^{ih_B t}\hat{O}e^{-ih_B t}$ .

We then turn to the solvent induced and vibration–solvent correlated effects on the EET system. Similar to Eq. (18), let us define

$$\begin{aligned} \varphi_{xy}(t) &\equiv i\langle[\hat{X}_B^B(t), \hat{Y}_B]\rangle_B = i\langle[\hat{Y}_B^B(t), \hat{X}_B]\rangle_B, \\ \varphi_{yy}(t) &\equiv i\langle[\hat{Y}_B^B(t), \hat{Y}_B]\rangle_B, \end{aligned} \quad (19)$$

and  $\tilde{\varphi}_{xy}(\omega)$  and  $\tilde{\varphi}_{yy}(\omega)$  are defined as Eq. (14). Note the second identity of Eq. (19) exists only in the current model. It is easy to verify that

$$\begin{aligned} \tilde{\varphi}_{xx}(0) &= \sum_k \frac{c_k^2}{\omega_k}, \\ \tilde{\varphi}_{xy}(0) &= \sum_k c_k d_k, \\ \tilde{\varphi}_{yy}(0) &= \sum_k \omega_k d_k^2. \end{aligned} \quad (20)$$

Thus  $\hat{F}_1$  of Eq. (7a) can now be recast as

$$\hat{F}_1 = D_1 \hat{q}, \quad (21)$$

with

$$D_1 = \tilde{\varphi}_{xy}(0) - [\Omega + \tilde{\varphi}_{xx}(0)]D. \quad (22)$$

We are now in the position to obtain  $\Phi_{ab}(t)$  of Eq. (13) via their frequency resolutions as long as the solvent response functions  $\varphi_{xx}(t)$ ,  $\varphi_{xy}(t)$ , and  $\varphi_{yy}(t)$  are known. From Eq. (21), together with Eqs. (15) and (16), we have immediately

$$\tilde{\Phi}_{11}(\omega) = D_1^2 \tilde{\chi}_{qq}(\omega). \quad (23)$$

Following the procedure of the establishment of the system–bath entanglement theorem in Ref. 46, we can further obtain

$$\begin{aligned} \tilde{\Phi}_{12}(\omega) &= \tilde{\Phi}_{21}(\omega) \\ &= D_1^{-1}[D\tilde{\varphi}_{xx}(\omega) - \tilde{\varphi}_{xy}(\omega)]\tilde{\Phi}_{11}(\omega), \end{aligned} \quad (24)$$

and

$$\begin{aligned} \tilde{\Phi}_{22}(\omega) &= D^2\tilde{\varphi}_{xx}(\omega) - 2D\tilde{\varphi}_{xy}(\omega) + \tilde{\varphi}_{yy}(\omega) \\ &+ D_1^{-1}[D\tilde{\varphi}_{xx}(\omega) - \tilde{\varphi}_{xy}(\omega)]\tilde{\Phi}_{12}(\omega). \end{aligned} \quad (25)$$

The detailed derivation for Eqs. (24) and (25) are given in Appendix A. Especially notice Eq. (A5) there that  $\Phi_{21}(t) = \Phi_{12}(t)$  in the current model. Hence all the involving  $\Phi_{ab}(t) = -\Phi_{ba}(-t)$  in Eq. (12) are odd functions, for  $a, b = 1, 2$ . The odd–function property leads to  $J_{ab}(\omega) = \text{Im}[\tilde{\Phi}_{ab}(\omega)]$ . They can then be readily obtained via Eqs. (23)–(25), together with the expression

of  $\tilde{\chi}_{qq}(\omega)$  [cf. Eq. (16)], as long as the solvent–space responses  $\tilde{\varphi}_{xx}(\omega)$ ,  $\tilde{\varphi}_{xy}(\omega)$ , and  $\tilde{\varphi}_{yy}(\omega)$  are known. The resulting  $J_{ab}(\omega)$ , characterizing the vibration–plus–solvent environment statistics, give the correlations  $C_{ab}(t)$  via Eq. (11), which will be plugged in the DEOM construction in Sec. III.

Combining Eqs. (23)–(25), the overall response function  $\Phi(t) \equiv i\langle[\hat{F}^{\text{env}}(t), \hat{F}^{\text{env}}(0)]\rangle_{\text{env}}$ , recast in term of the frequency resolution as

$$\tilde{\Phi}(\omega) = \sum_{ab} \tilde{\Phi}_{ab}(\omega), \quad (26)$$

is finally obtained as

$$\begin{aligned} \tilde{\Phi}(\omega) &= D^2\tilde{\varphi}_{xx}(\omega) - 2D\tilde{\varphi}_{xy}(\omega) + \tilde{\varphi}_{yy}(\omega) \\ &+ [D_1 + D\tilde{\varphi}_{xx}(\omega) - \tilde{\varphi}_{xy}(\omega)]^2 \tilde{\chi}_{qq}(\omega). \end{aligned} \quad (27)$$

Similarly, denote

$$J(\omega) = \text{Im}\tilde{\Phi}(\omega) = \sum_{ab} J_{ab}(\omega). \quad (28)$$

The second identity is referred from Eq. (12) and the fact that  $\Phi(t)$  is an odd function. The overall reorganization energy is related to the overall response resolution  $\tilde{\Phi}(\omega)$  via[21]

$$\lambda = \frac{1}{2\pi} \int_{-\infty}^{\infty} d\omega \frac{J(\omega)}{\omega} = \frac{1}{2} \tilde{\Phi}(0). \quad (29)$$

It recovers the expression of  $\lambda$  in Eq. (5) by substituting Eqs. (16) and (20) into Eq. (27) for  $\omega = 0$ .

### III. DEOM FORMALISM

With the overall environment influence response function [cf. Eq. (27)] obtained, the EET dynamics and spectra can be simulated via the DEOM approach. DEOM has been applied to study the Herzberg–Teller vibronic coupling in our previous work.[18] But the correlated non-polarized solvent effects were not included there. In this section we will give a general DEOM construction in the existence of correlated polarized and non-polarized environments.

#### A. The system–plus–environment Hamiltonian

For generality, let us recast the total Hamiltonian of Eq. (1) into the system–plus–environment form as [cf. Eqs. (5) and (6)]

$$H_T(t) = H_{\text{ex}} + H_{\text{env}} + \sum_{a=1,2} \hat{Q}_a \hat{F}_a - \hat{\mu}_T \varepsilon(t), \quad (30)$$

with

$$H_{\text{ex}} = (\Delta + \lambda) \hat{B}^\dagger \hat{B}, \quad (31)$$

and

$$\hat{Q}_1 = \hat{Q}_2 = \hat{B}^\dagger \hat{B}. \quad (32)$$

The form of separated  $\hat{F}_1$  and  $\hat{F}_2$  (as well as  $\hat{Q}_1$  and  $\hat{Q}_2$  although they are equal) has to be adopted for the later DEOM simulation due to the fact that they may participate differently in the total dipole moment. In this work the vibration is considered of optical polarization while the solvent not. The total dipole moment operator assumes the form in the Herzberg–Teller approximation as

$$\hat{\mu}_T = \sum_{a=1,2} \hat{D}_a (u_a + v_a \hat{F}_a), \quad (33)$$

with

$$\hat{D}_1 = \hat{B}^\dagger + \hat{B}, \quad u_1 = \mu_{\text{ex}}, \quad v_1 = \nu_{\text{vib}}, \quad (34a)$$

for the non-Condon vibronic coupling mode, while

$$\hat{D}_2 = 0 \quad \text{and} \quad u_2 = v_2 = 0, \quad (34b)$$

for the non-polarized solvent.  $\mu_{\text{ex}}$  and  $\nu_{\text{vib}}$  characterize the excitonic system dipole strength and the non-Condon vibronic coupling strength, respectively.  $\varepsilon(t)$  in Eq. (30) is the classical external field. Generally, DEOM theory deal with arbitrary  $H_{\text{ex}}$ ,  $\{\hat{Q}_a\}$ , and  $\{\hat{D}_a\}$ . Influences of  $\{\hat{F}_a\}$  are exerted via their correlation functions  $\{C_{ab}(t)\}$  in the environmental space. The  $\hat{F}_1$  and  $\hat{F}_2$  are associate with the intramolecular vibrational mode and the solvent degrees of freedom, respectively, as given in Eqs. (7) with (8). Their participations will be treated in a unified way in the DEOM formalism, see the following subsections, although the vibrational mode is optically polarizable, while the solvent not. Their difference in the optical activity is reflected just via setting the parameters,  $u_a$  and  $v_a$ , cf. Eqs. (34). Their correlated overall environmental statistical properties have been derived in the previous section. The key results are give in Eqs. (23)–(25), in terms of the bath interaction response functions. The bath correlation functions, on basis of which the DEOM is constructed, are obtained via the the fluctuation–dissipation theorem, Eq. (11).

## B. Bath correlations

The DEOM construction starts with an exponential expansion of correlation function satisfying Eq. (11) as

$$\langle \hat{F}_a^{\text{env}}(t) \hat{F}_b^{\text{env}}(0) \rangle_{\text{env}} = \sum_j \eta_{abj} e^{-\gamma_{abj} t}. \quad (35)$$

This can generally be achieved via certain sum–over–poles expansion on the Fourier integrand of Eq. (11), followed by the Cauchy’s contour integration in the low–half plane. Poles arising from the Bose function,  $1/(1-e^{-\beta\omega})$ , are all real, while those from  $J_{ab}(\omega)$  are either real or complex–conjugate paired. Define the associated index  $\bar{j}$

via  $\gamma_{ab\bar{j}} \equiv \gamma_{abj}^*$ , that must also be an exponent of Eq. (35). Due to the time–reversal relation,  $\langle \hat{F}_b^{\text{env}}(0) \hat{F}_a^{\text{env}}(t) \rangle_{\text{B}} = \langle \hat{F}_a^{\text{env}}(t) \hat{F}_b^{\text{env}}(0) \rangle_{\text{B}}^*$ , we have

$$\langle \hat{F}_b^{\text{env}}(0) \hat{F}_a^{\text{env}}(t) \rangle_{\text{env}} = \sum_j \eta_{ab\bar{j}}^* e^{-\gamma_{abj} t}. \quad (36)$$

For convenience in the later DEOM construction, we recast Eqs. (35) and (36) as

$$\begin{aligned} \langle \hat{F}_a^{\text{env}}(t) \hat{F}_b^{\text{env}}(0) \rangle_{\text{env}} &= \sum_{\kappa} \eta_{ab\kappa} e^{-\gamma_{\kappa} t}, \\ \langle \hat{F}_b^{\text{env}}(0) \hat{F}_a^{\text{env}}(t) \rangle_{\text{env}} &= \sum_{\kappa} \eta_{ab\bar{\kappa}}^* e^{-\gamma_{\kappa} t}. \end{aligned} \quad (37)$$

Here,  $\gamma_{\kappa}$  runs over all involved exponents in  $\{\gamma_{abj}\}$  but with  $\eta_{ab\kappa}$  or  $\eta_{ab\bar{\kappa}}^*$  being zero if not really among the terms in Eq. (35) or Eq. (36).

## C. Dissipaton algebra and the construction of DEOM

The dissipaton decomposition on the hybridization environment operator reads[40, 42]

$$\hat{F}_a^{\text{env}} = \sum_{\kappa} \hat{f}_{a\kappa}. \quad (38)$$

This decomposition recovers Eqs. (37), by assuming that dissipatons are statistically independent, with their correlation functions ( $t > 0$ )

$$\begin{aligned} \langle \hat{f}_{a\kappa}(t) \hat{f}_{b\kappa'}(0) \rangle_{\text{env}} &= \delta_{\kappa\kappa'} \eta_{ab\kappa} e^{-\gamma_{\kappa} t}, \\ \langle \hat{f}_{b\kappa'}(0) \hat{f}_{a\kappa}(t) \rangle_{\text{env}} &= \delta_{\kappa\kappa'} \eta_{ab\bar{\kappa}}^* e^{-\gamma_{\kappa} t}. \end{aligned} \quad (39)$$

These lead to the generalized diffusion equation reading

$$\text{tr}_{\text{env}} \left[ \left( \frac{\partial}{\partial t} \hat{f}_{a\kappa} \right)_{\text{env}} \rho_{\text{T}}(t) \right] = -\gamma_{\kappa} \text{tr}_{\text{env}} [\hat{f}_{a\kappa} \rho_{\text{T}}(t)]. \quad (40)$$

In the DEOM construction below, this will be used together with the Heisenberg equation–of–motion in the bare environment,

$$\left( \frac{\partial}{\partial t} \hat{f}_{a\kappa} \right)_{\text{env}} = -i[\hat{f}_{a\kappa}, H_{\text{env}}]. \quad (41)$$

The dynamical variables in DEOM are called the dissipaton density operators (DDOs), defined as:

$$\rho_{\mathbf{n}}^{(n)}(t) \equiv \text{tr}_{\text{env}} \left[ \left( \prod_{a\kappa} \hat{f}_{a\kappa}^{n_{a\kappa}} \right)^{\circ} \rho_{\text{T}}(t) \right]. \quad (42)$$

Here,  $n = \sum_{a\kappa} n_{a\kappa}$  and  $\mathbf{n} = \{n_{a\kappa}\}$  that is an ordered set of the occupation numbers,  $n_{a\kappa} = 0, 1, \dots$ , on individual dissipatons. The circled parentheses,  $(\dots)^{\circ}$ , is irreducible notation. For bosonic dissipatons it follows that  $(\hat{f}_{a\kappa} \hat{f}_{b\kappa'})^{\circ} = (\hat{f}_{b\kappa'} \hat{f}_{a\kappa})^{\circ}$ .

The key ingredient in the dissipaton algebra is the generalized Wick's theorem:

$$\begin{aligned} & \text{tr}_{\text{env}} \left[ \left( \prod_{a\kappa} \hat{f}_{a\kappa}^{n_{a\kappa}} \right)^\circ \hat{f}_{b\kappa'} \rho_{\text{T}}(t) \right] \\ &= \rho_{\mathbf{n}_{b\kappa'}^+}^{(n+1)}(t) + \sum_{a\kappa} n_{a\kappa} \langle \hat{f}_{a\kappa} \hat{f}_{b\kappa'} \rangle_{\text{env}}^{\rho_{\mathbf{n}_{a\kappa}^-}^{(n-1)}}(t), \end{aligned} \quad (43a)$$

and

$$\begin{aligned} & \text{tr}_{\text{env}} \left[ \left( \prod_{a\kappa} \hat{f}_{a\kappa}^{n_{a\kappa}} \right)^\circ \rho_{\text{T}}(t) \hat{f}_{b\kappa'} \right] \\ &= \rho_{\mathbf{n}_{b\kappa'}^+}^{(n+1)}(t) + \sum_{a\kappa} n_{a\kappa} \langle \hat{f}_{b\kappa'} \hat{f}_{a\kappa} \rangle_{\text{env}}^{\rho_{\mathbf{n}_{a\kappa}^-}^{(n-1)}}(t). \end{aligned} \quad (43b)$$

Here,  $\mathbf{n}_{a\kappa}^\pm$  differs from  $\mathbf{n}$  only at the specified  $\hat{f}_{a\kappa}$ -dissipaton occupation number,  $n_{a\kappa}$ , by  $\pm 1$  and

$$\begin{aligned} \langle \hat{f}_{a\kappa} \hat{f}_{b\kappa'} \rangle_{\text{env}}^{\rho_{\mathbf{n}_{a\kappa}^-}^{(n-1)}} &\equiv \langle \hat{f}_{a\kappa}(0+) \hat{f}_{b\kappa'}(0) \rangle_{\text{env}} = \eta_{ab\kappa} \delta_{\kappa\kappa'}, \\ \langle \hat{f}_{b\kappa'} \hat{f}_{a\kappa} \rangle_{\text{env}}^{\rho_{\mathbf{n}_{a\kappa}^-}^{(n-1)}} &\equiv \langle \hat{f}_{b\kappa'}(0) \hat{f}_{a\kappa}(0+) \rangle_{\text{env}} = \eta_{ab\bar{\kappa}}^* \delta_{\kappa\kappa'}. \end{aligned} \quad (44)$$

The DEOM can now be readily constructed by applying  $\dot{\rho}_{\text{T}}(t) = -i[H_{\text{T}}(t), \rho_{\text{T}}(t)]$ , to the total composite density operator in Eq. (42); i.e.,

$$\dot{\rho}_{\mathbf{n}}^{(n)}(t) = -i \text{tr}_{\text{env}} \left\{ \left( \prod_{a\kappa} \hat{f}_{a\kappa}^{n_{a\kappa}} \right)^\circ [H_{\text{T}}(t), \rho_{\text{T}}(t)] \right\}. \quad (45)$$

To proceed, let us recast the total Hamiltonian, Eq. (30) with Eqs. (33) and (38), as

$$\begin{aligned} H_{\text{T}}(t) &= \left[ H_{\text{ex}} - \sum_a \mu_a \hat{D}_a \varepsilon(t) \right] + H_{\text{env}} \\ &+ \sum_{a\kappa} [\hat{Q}_a - v_a \hat{D}_a \varepsilon(t)] \hat{f}_{a\kappa}. \end{aligned} \quad (46)$$

Using Eq. (40) with Eq. (41) for the action of  $H_{\text{env}}$ , and Eqs. (43)–(44) for the action of the last term in Eq. (46), we obtain from Eq. (45) the DEOM reading

$$\begin{aligned} \dot{\rho}_{\mathbf{n}}^{(n)} &= - \left[ i\mathcal{L}(t) + \sum_{a\kappa} n_{a\kappa} \gamma_{\kappa} \right] \rho_{\mathbf{n}}^{(n)} - i \sum_{a\kappa} \tilde{\mathcal{A}}_a(t) \rho_{\mathbf{n}_{a\kappa}^+}^{(n+1)} \\ &- i \sum_{a\kappa} n_{a\kappa} \tilde{\mathcal{C}}_{a\kappa}(t) \rho_{\mathbf{n}_{a\kappa}^-}^{(n-1)}. \end{aligned} \quad (47)$$

Here, the involved superoperators are

$$\mathcal{L}(t) \hat{O} \equiv \mathcal{L}_{\text{ex}} \hat{O} - \varepsilon(t) \sum_a u_a \mathcal{V}_a \hat{O}, \quad (48a)$$

and

$$\tilde{\mathcal{A}}_a(t) \hat{O} \equiv \mathcal{A}_a \hat{O} - \varepsilon(t) v_a \mathcal{V}_a \hat{O}, \quad (48b)$$

$$\tilde{\mathcal{C}}_{a\kappa}(t) \hat{O} \equiv \mathcal{C}_{a\kappa} \hat{O} - \varepsilon(t) \mathcal{D}_{a\kappa} \hat{O}. \quad (48c)$$

with the field-free superoperators

$$\mathcal{L}_{\text{ex}} \hat{O} \equiv [H_{\text{ex}}, \hat{O}], \quad \mathcal{V}_a \hat{O} \equiv [\hat{D}_a, \hat{O}], \quad \mathcal{A}_a \hat{O} \equiv [\hat{Q}_a, \hat{O}], \quad (49a)$$

and

$$\mathcal{C}_{a\kappa} \hat{O} \equiv \sum_b (\eta_{ab\kappa} \hat{Q}_b \hat{O} - \eta_{ab\bar{\kappa}}^* \hat{O} \hat{Q}_b), \quad (49b)$$

$$\mathcal{D}_{a\kappa} \hat{O} \equiv \sum_b v_b (\eta_{ab\kappa} \hat{D}_b \hat{O} - \eta_{ab\bar{\kappa}}^* \hat{O} \hat{D}_b). \quad (49c)$$

Equations (47)–(49) constitute the final DEOM formalism for the hybridized dynamics of system and its environment, coupled to external fields on Herzberg–Teller polarization [cf. Eq. (33)].

#### D. Entangled system–and–environment polarization

In this subsection, we elaborate the procedure to evaluate the entangled system–and–environment polarization via DEOM. Consider the total polarization,

$$P_{\text{T}}(t) = \text{Tr}[\hat{\mu}_{\text{T}} \rho_{\text{T}}(t)] = \text{tr}_{\text{S}} \text{tr}_{\text{env}} [\hat{\mu}_{\text{T}} \rho_{\text{T}}(t)]. \quad (50)$$

Here [cf. Eqs. (33) and (38)],

$$\hat{\mu}_{\text{T}} = \sum_a \hat{D}_a (u_a + v_a \sum_{\kappa} \hat{f}_{a\kappa}). \quad (51)$$

With Eq. (42), the dissipaton–space evaluation on the Herzberg–Teller polarization can be expressed as

$$P_{\text{T}}(t) = \sum_a \text{tr}_{\text{S}} \left\{ \hat{D}_a \left[ u_a \rho^{(0)}(t) + v_a \sum_{\kappa} \rho_{a\kappa}^{(1)}(t) \right] \right\}. \quad (52)$$

The involved  $\rho^{(0)}(t)$  and  $\{\rho_{a\kappa}^{(1)}(t)\}$  are propagated via Eq. (47) with the dressing field.

Focusing on the linear absorption spectra, one can also evaluate the dipole–dipole correlation function in the scenario as

$$\langle \hat{\mu}_{\text{T}}(t) \hat{\mu}_{\text{T}}(0) \rangle \equiv \text{Tr}(\hat{\mu}_{\text{T}} e^{-i\mathcal{L}_{\text{M}} t} \hat{\mu}_{\text{T}} \rho_{\text{T}}^{\text{eq}}). \quad (53)$$

Here,  $\mathcal{L}_{\text{M}} \cdot \equiv [H_{\text{M}}, \cdot]$  and  $\rho_{\text{T}}^{\text{eq}} = |0\rangle\langle 0| e^{-\beta H_{\text{env}}} / \text{Tr} e^{-\beta H_{\text{env}}}$  are the total composite field-free matter Liouvillian and the thermal equilibrium density operator, respectively, cf. Eq. (1b). The evaluation on the dipole–dipole correlation function via DEOM goes with the following steps for general cases.

1. Determine the steady–state correspondence of  $\rho_{\text{T}}^{\text{eq}} \Rightarrow \{\rho_{\mathbf{n};\text{eq}}^{(n)}\}$  evaluated as the solutions to  $\dot{\rho}_{\mathbf{n}}^{(n)} = 0$  of the field-free Eq. (47). [47, 48] For general systems, a self-consistent iteration approach has been proposed to efficiently solve this problem. [49]
2. Identify the correspondence  $\hat{\mu}_{\text{T}} \rho_{\text{T}}^{\text{eq}} \Rightarrow \{\rho_{\mathbf{n}}^{(n)}(t) = 0; \hat{\mu}_{\text{T}}\}$  by using Eq. (42). We obtain

$$\begin{aligned} \rho_{\mathbf{n}}^{(n)}(t=0; \hat{\mu}_{\text{T}}) &\equiv \text{tr}_{\text{env}} \left[ \left( \prod_{a\kappa} \hat{f}_{a\kappa}^{n_{a\kappa}} \right)^\circ (\hat{\mu}_{\text{T}} \rho_{\text{T}}^{\text{eq}}) \right] \\ &= \sum_a \hat{D}_a \left( u_a \rho_{\mathbf{n};\text{eq}}^{(n)} + v_a \sum_{\kappa} \hat{\rho}_{\mathbf{n}_{a\kappa}^+;\text{eq}}^{(n+1)} \right) \\ &+ \sum_{ab\kappa} v_b n_{a\kappa} \eta_{ab\kappa} \hat{D}_b \rho_{\mathbf{n}_{a\kappa}^-;\text{eq}}^{(n-1)}. \end{aligned} \quad (54)$$

The second identity is obtained by using Eq. (51) for  $\hat{\mu}_T$ , followed by the generalized Wick's theorem, Eq. (43a) with Eq. (44). It can also be viewed as the left-action of dipole operator onto the DDOs in the DEOM, Eqs. (47)–(49).

3. The field-free DEOM propagation is then followed to obtain  $\{\rho_{\mathbf{n}}^{(n)}(t; \hat{\mu}_T)\}$ , the DEOM-space correspondence to  $e^{-i\mathcal{L}_M t}(\hat{\mu}_T \rho_{\mathbf{n}}^{\text{eq}})$ .
4. Calculate Eq. (53) in terms of the expectation value like Eq. (52); i.e.,

$$\langle \hat{\mu}_T(t) \hat{\mu}_T(0) \rangle = \sum_a u_a \text{tr}_s \left[ \hat{D}_a \rho^{(0)}(t; \hat{\mu}_T) \right] + \sum_a v_a \text{tr}_s \left[ \hat{D}_a \sum_{\kappa} \rho_{a\kappa}^{(1)}(t; \hat{\mu}_T) \right]. \quad (55)$$

Finally, the linear absorption spectrum of the total matter is transformed as

$$S_A(\omega) = \text{Re} \int_0^\infty dt e^{i\omega t} \langle \hat{\mu}_T(t) \hat{\mu}_T(0) \rangle. \quad (56)$$

#### IV. NUMERICAL DEMONSTRATION

For the numerical demonstration, we apply Drude model for the solvent responses  $\tilde{\varphi}_{xx}(\omega)$ ,  $\tilde{\varphi}_{xy}(\omega)$ , and  $\tilde{\varphi}_{yy}(\omega)$ , i.e.

$$\tilde{\varphi}_{cc'}(\omega) = \frac{2\eta_{cc'}\gamma}{\gamma - i\omega}, \quad (57)$$

with  $c, c' = x, y$ .  $\{\eta_{cc'}\}$  are real and non-negative parameters which satisfy

$$\eta_{xx}^2 \leq \eta_{xx}\eta_{yy}. \quad (58)$$

We introduce further two dimensionless factors to reflect the relations among them:

$$g_1 \equiv \eta_{xy}/(D\eta_{xx}) \quad \text{and} \quad g_2 \equiv (D\eta_{xy})/\eta_{yy}. \quad (59)$$

The relation Eq. (58) requires  $g_1 g_2 \leq 1$ . The total transition dipole moments takes the form of Eq. (33) with Eq. (34). Inferred from Eq. (C28), we set

$$\mu_{\text{vib}} \equiv \Omega \nu_{\text{vib}}, \quad (60)$$

to characterize the strength of the vibrational dipole moment. We select three types of cases for the following demonstrations.

1. Brownian-vibration cases:  $g_1 = g_2 = 1$ . It leads to  $\tilde{\Phi}_{12}(\omega) = \tilde{\Phi}_{21}(\omega) = \tilde{\Phi}_{22}(\omega) = 0$  [cf. Eqs. (24) and (25)], whereas

$$\tilde{\Phi}_{11}(\omega) = \Omega^2 D^2 \tilde{\chi}_{qq}(\omega), \quad (61)$$

as inferred from Eqs. (22) and (23). Here the vibrational mode in the solvent behaves as a Brownian oscillator. While the solvent will not directly affect the EET dynamics.

2. Un-synergetic vibration-solvent cases:  $g_1 = 1$  but  $g_2 \neq 1$ . This results in  $\tilde{\Phi}_{12}(\omega) = \tilde{\Phi}_{21}(\omega) = 0$  and

$$\tilde{\Phi}_{11}(\omega) = \Omega^2 D^2 \tilde{\chi}_{qq}(\omega), \quad (62a)$$

$$\tilde{\Phi}_{22}(\omega) = (1 - g_2) \tilde{\varphi}_{yy}(\omega). \quad (62b)$$

In the following demonstrations, these conditions will be called ‘‘un-synergetic’’ to specifically refer to the cases that the environmental cross-response and correlation functions between the Brownian vibrational mode and the diffusive solvent vanish.

3. General correlated vibration-solvent cases:  $g_1 \neq 1$  and  $g_2 \neq 1$ . These are general cases with all the environment influence components, Eqs. (23)–(25), being nonzero.

Analytic solution can be derived for the linear absorption of the monomer system studied in this work. With the derivation detailed in Appendix B, the final result is summarized as follows.

$$\langle \hat{\mu}_T(t) \hat{\mu}_T(0) \rangle = e^{-i(\Delta+\lambda)t} e^{-g(t)}, \quad (63a)$$

with

$$e^{-g(t)} = \left[ \left( \mu_{\text{ex}} - i\nu_{\text{vib}} \int_0^t d\tau \langle \hat{F}_1^{\text{env}}(\tau) \hat{F}_1^{\text{env}}(0) \rangle \right) \times \left( \mu_{\text{ex}} - i\nu_{\text{vib}} \int_0^t d\tau \langle \hat{F}_1^{\text{env}}(\tau) \hat{F}_1^{\text{env}}(0) \rangle \right) + \nu_{\text{vib}}^2 \langle \hat{F}_1^{\text{env}}(t) \hat{F}_1^{\text{env}}(0) \rangle \right] e^{-g_0(t)}, \quad (63b)$$

and

$$g_0(t) = \int_0^t d\tau \int_0^\tau d\tau' \langle \hat{F}_1^{\text{env}}(\tau) \hat{F}_1^{\text{env}}(\tau') \rangle. \quad (63c)$$

Expressions in the gas-phase condition are further derived in Appendix C, via two distinct methods. Given there is also the zero-temperature limit. The numerical DEOM results, obtained via the procedure described in Sec. III D, via DDOs, have all been confirmed to be consistent with the analytic solutions, and exhibited in Fig. 1. Note that in the present simulations, the step No.1 in Sec. III D can actually be skipped since the EET system is initially thermally equilibrated at the ground electronic state.

Figure 1 depicts the monomer absorption spectra in the Brownian-vibration, un-synergetic, and general correlated vibration-solvent cases at different temperatures, with various Huang-Rhys factors,  $S = D^2/2$ , and vibrational dipole strengths  $\mu_{\text{vib}}$  [cf. Eq. (60)]. We select  $\Delta = 10000\text{cm}^{-1}$  and  $\Omega = 200\text{cm}^{-1}$ . Other parameters are indicated in the figure or given in the caption. For the polarized vibronic degree of freedom,  $\hat{F}_1$ , which behaves as a Brownian oscillator under the influence of solvent, the effective frequency has been analyzed in Ref. 50 to be

$$\Omega_{\text{eff}}^2 = \lim_{t \rightarrow \infty} \frac{\ddot{\chi}_{qq}^2(t) - \ddot{\chi}_{qq}(t)\dot{\chi}_{qq}(t)}{\dot{\chi}_{qq}^2(t) - \ddot{\chi}_{qq}(t)\chi_{qq}(t)}, \quad (64)$$

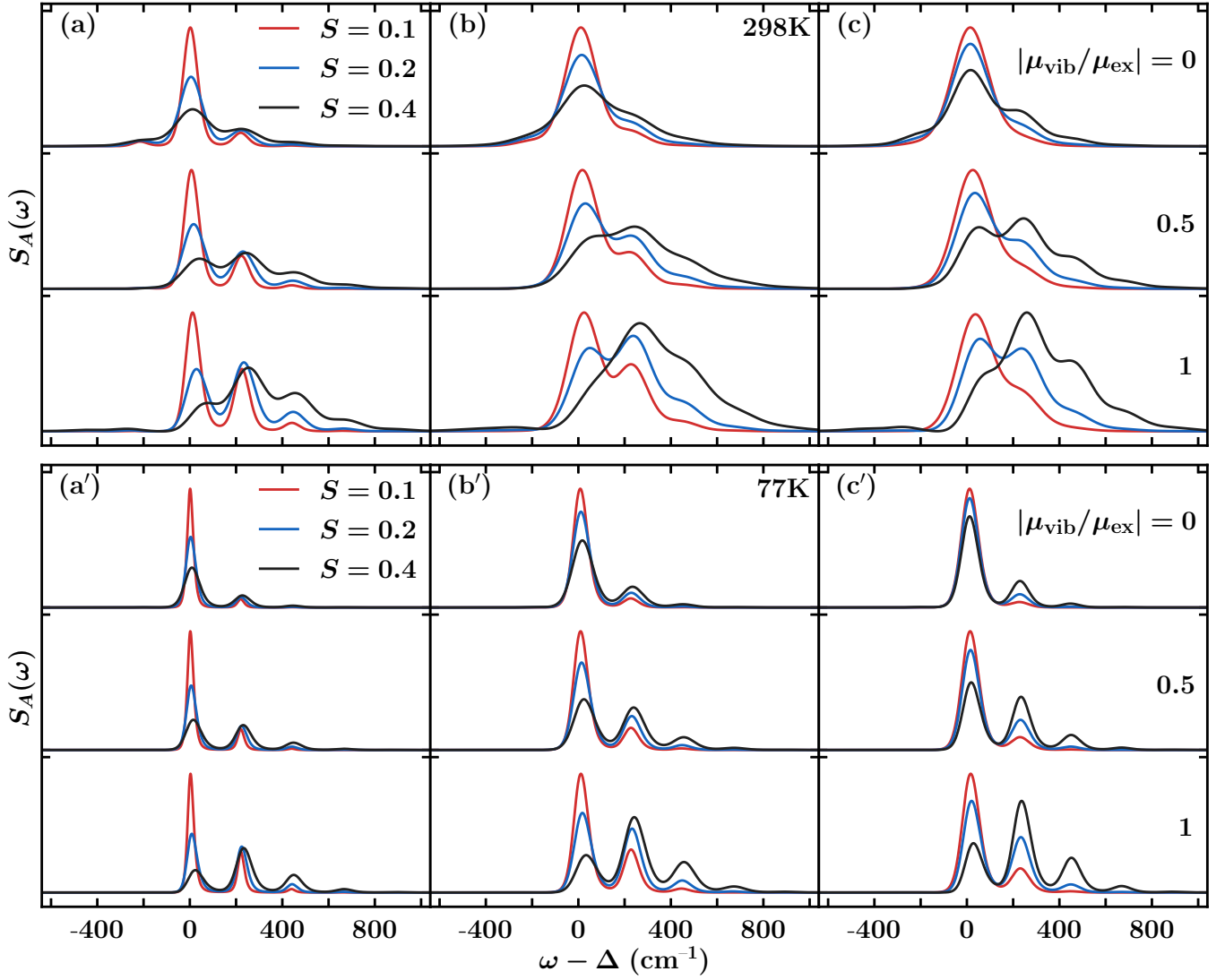


FIG. 1: Linear absorption lineshapes at the temperatures  $T = 298\text{K}$  [upper panels, (a), (b), and (c)] and  $T = 77\text{K}$  [lower panels, (a'), (b'), and (c')], in the cases of Brownian-vibration [left panels, (a) and (a')], un-synergetic vibration-solvent [middle panels, (b) and (b')], and general correlated vibration-solvent [right panels, (c) and (c')]. Huang-Rhys factors are selected as  $S = 0.1, 0.2, 0.4$  with different vibrational dipole strengths,  $|\mu_{\text{vib}}/\mu_{\text{ex}}| = 0, 0.5, 1$ . For the un-synergetic vibration-solvent case, we select  $g_2 = 0.5$ ; whereas for the general correlated vibration-solvent case, we choose  $g_2 = g_1^{-1} = \sqrt{2S}$ . The other parameters are:  $\Delta = 10000\text{cm}^{-1}$ ,  $\Omega = 200\text{cm}^{-1}$ , and  $\gamma = \eta_{xx} = 20\text{cm}^{-1}$ .

with  $\chi_{qq}(t)$  being defined in Eq. (15). It characterizes the spectroscopic features in Fig. 1, rather than the original frequency  $\Omega$ . Based on the selected solvent parameters, the  $\Omega_{\text{eff}}$  is obtained to be  $1.095\Omega$ . We can see that the solvent effect is more important at high temperature than at low temperature, by comparison to the corresponding gas-phase results, depicted in Fig. 3 in Appendix C. The solvent broadening is observed by comparing (b) to (a) and the coherence enhancement, due to the synergetic vibration-solvent correlation, is observed by comparing (c) to (b).

Figure 2 shows the strong field induced polarization spectra,

$$\tilde{P}(\omega) \equiv \int_{-\infty}^{\infty} dt e^{i\omega t} [P_{\text{T}}(t) - P_{\text{T}}^{\text{eq}}], \quad (65)$$

evaluated via the DEOM simulations.  $P_{\text{T}}^{\text{eq}}$  is the equilibrium polarization of the total system. Right-hand-sides of the break exhibit the nonlinear triple-frequency signals. The external field is adopted as a Gaussian pulse, with the envelope being

$$\mu_{\text{ex}}\varepsilon(t) = \frac{\theta}{\sqrt{2\pi}\sigma} \exp\left(-\frac{t^2}{2\sigma^2}\right) \cos(\omega_0 t). \quad (66)$$

Here,  $\omega_0$  is the carrier frequency.  $\theta$  and  $\sigma$  denotes the pulse strength and width. We set  $\omega_0 = 10040\text{cm}^{-1}$  and  $\sigma = 4$  fs.  $\theta$  is chosen as  $0.1\pi$  (upper panels) and  $0.5\pi$  (lower panels), for the relative weak and strong dressing fields, respectively. Both the nonlinear polarization and the dressed effect in the linear regime vanish in the weak field limit, as indicated in the upper panels. Similar to Fig. 1, the (b) and (b') panels in Fig. 2 exhibit the solvent

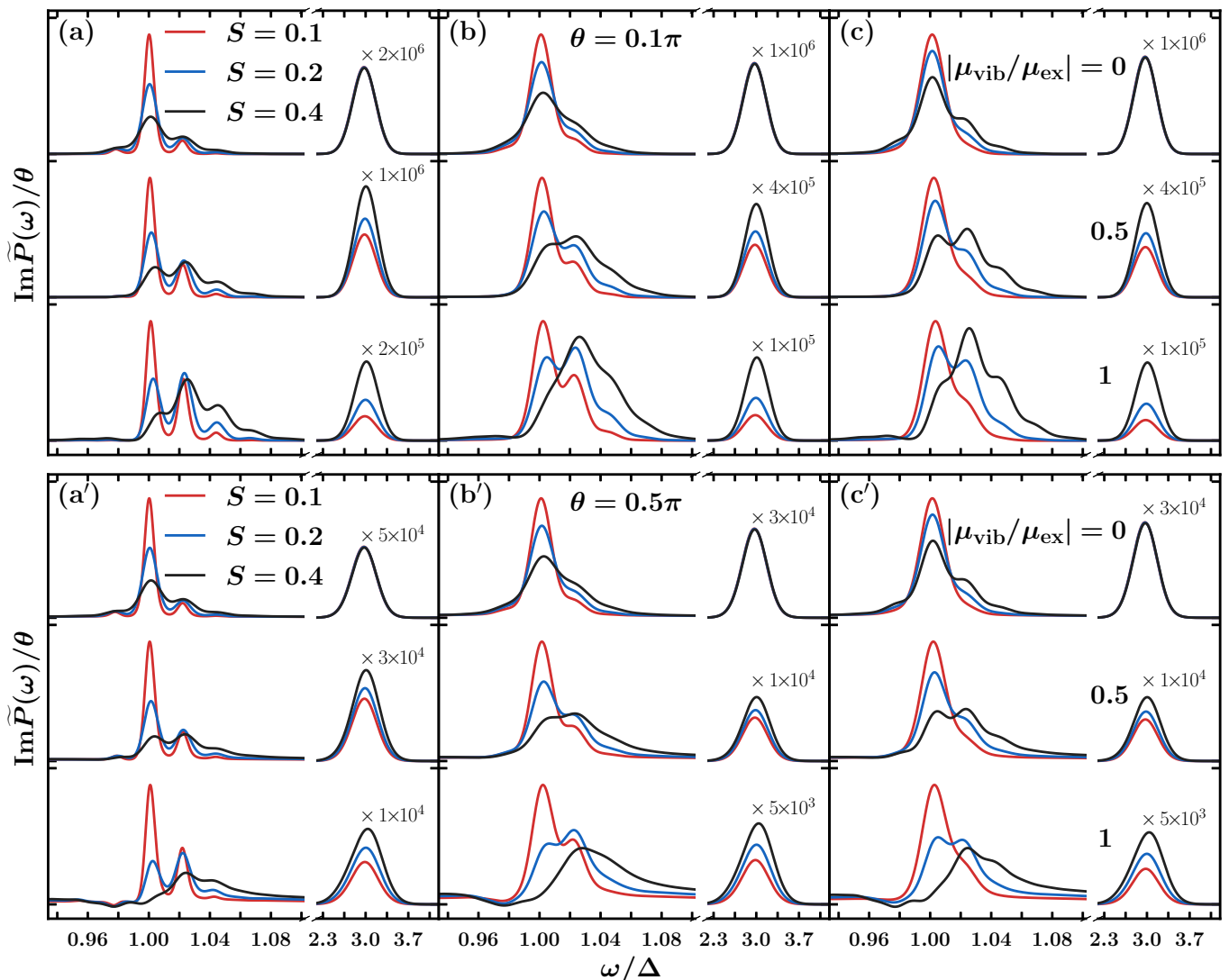


FIG. 2: Strong field induced polarization spectra (scaled by the flipping angle  $\theta$ ) for  $\theta = 0.1\pi$  [upper panels, (a), (b), and (c)] and  $\theta = 0.5\pi$  [lower panels, (a'), (b'), and (c')] at  $T = 298\text{K}$ , in the cases of Brownian-vibration [left panels, (a) and (a')], un-synergetic vibration-solvent [middle panels, (b) and (b')], and general correlated vibration-solvent [right panels, (c) and (c')]. Other parameters are same as in Fig. 1.

broadening effect in comparison to the (a) and (a') panels; whereas the (c) and (c') panels show the synergetic vibration-solvent correlation induced coherence enhancement in comparison to the (b) and (b') panels.

## V. SUMMARY

To summarize, this work studies the correlated effect between the non-Condon vibronic coupling and the surrounding solvent influences. We start from a physical monomer model which involves correlated exciton-vibration, exciton-solvent, and vibration-solvent interactions, with both the exciton and the vibrational mode being optical polarizable. The overall statistical vibration-plus-solvent environmental effects are analyzed detailedly in obtaining the overall environmental interaction response functions. On basis of

them, we derive the analytic linear absorption solutions and construct the general dissipaton-equation-of-motion (DEOM) formalism to carry out simulations on nonlinear spectroscopies and arbitrary systems. Numerical demonstrations in either the linear absorption or strong field regime clearly show the coherence enhancement due to the synergetic vibration-solvent correlation. This observed feature is expected to be detected in the multi-exciton systems and multi-dimensional spectroscopies as well. The solvent-polarization induced Fano interference is also to be considered in future work.

**Data Availability:** The data that support the findings of this study are available from the corresponding author upon reasonable request.



## Acknowledgments

Support from the Ministry of Science and Technology of China No. 2017YFA0204904, the National Natural Science Foundation of China No. 21633006, and Anhui Initiative in Quantum Information Technologies is gratefully acknowledged.

### Appendix A: Derivation for Eqs. (24)–(25)

Note that in the present microscopic model,

$$\varphi_{xx}(t) = \sum_k c_k^2 \sin(\omega_k t), \quad (\text{A1a})$$

$$\varphi_{xy}(t) = \sum_k \omega_k c_k d_k \sin(\omega_k t), \quad (\text{A1b})$$

$$\varphi_{yy}(t) = \sum_k \omega_k^2 d_k^2 \sin(\omega_k t). \quad (\text{A1c})$$

From Eq. (10) together with Eq. (2), we have

$$\ddot{\hat{x}}_k^{\text{env}}(t) = -\omega_k^2 \hat{x}_k^{\text{env}}(t) + \omega_k c_k \hat{q}^{\text{env}}(t). \quad (\text{A2})$$

The formal solution to  $\hat{x}_k^{\text{env}}(t)$  is

$$\begin{aligned} \hat{x}_k^{\text{env}}(t) &= \hat{x}_k \cos(\omega_k t) + \hat{p}_k \sin(\omega_k t) \\ &+ c_k \int_0^t d\tau \sin[\omega_k(t - \tau)] \hat{q}^{\text{env}}(\tau). \end{aligned} \quad (\text{A3})$$

Together with Eq. (8), the above equation leads to

$$\hat{X}_B^{\text{env}}(t) = \hat{X}_B^{\text{B}}(t) + \int_0^t d\tau \varphi_{xx}(t - \tau) \hat{q}^{\text{env}}(\tau), \quad (\text{A4a})$$

$$\hat{Y}_B^{\text{env}}(t) = \hat{Y}_B^{\text{B}}(t) + \int_0^t d\tau \varphi_{xy}(t - \tau) \hat{q}^{\text{env}}(\tau). \quad (\text{A4b})$$

As  $[\hat{X}_B^{\text{B}}(t), \hat{O}] = [\hat{Y}_B^{\text{B}}(t), \hat{O}] = 0$  for arbitrary vibrational operator  $\hat{O}$ , we obtain [cf. Eqs. (7) and (21)]

$$\begin{aligned} \Phi_{21}(t) &= D_0^{-1} \int_0^t d\tau [D\varphi_{xx}(t - \tau) - \varphi_{xy}(t - \tau)] \Phi_{11}(\tau) \\ &= \Phi_{12}(t). \end{aligned} \quad (\text{A5})$$

The second identity is obtained by  $\Phi_{12}(t) = -\Phi_{21}(-t)$ , together with the fact that  $\Phi_{\text{vib}}(t)$ ,  $\varphi_{xx}(t)$ ,  $\varphi_{xy}(t)$  are all odd functions. Furthermore, Eqs. (A4) together with Eq. (7b) result in

$$\begin{aligned} \Phi_{22}(t) &= D_0^{-1} \int_0^t d\tau [D\varphi_{xx}(t - \tau) - \varphi_{xy}(t - \tau)] \Phi_{12}(\tau) \\ &+ D^2 \varphi_{xx}(t) - 2D\varphi_{xy}(t) + \varphi_{yy}(t). \end{aligned} \quad (\text{A6})$$

In terms of frequency resolution, Eq. (A5) and Eq. (A6) lead to Eq. (24) and Eq. (25), respectively.

## Appendix B: Derivation of Eq. (63)

This appendix derives the analytic linear absorption lineshape in case of non-Condon polarization. For the monomer system in this work, the dipole–dipole correlation, Eq. (53), can be recast as [cf. Eq. (33) with Eq. (34)]

$$\begin{aligned} \langle \hat{\mu}_T(t) \hat{\mu}_T(0) \rangle &= e^{-i\Delta t} \langle e^{iH_{\text{env}} t} (\mu_{\text{ex}} + \nu_{\text{vib}} \hat{F}_1) e^{-iH_{\text{env}} t} \\ &\quad \times (\mu_{\text{ex}} + \nu_{\text{vib}} \hat{F}_1) \rangle. \end{aligned} \quad (\text{B1})$$

By applying [cf. Eq. (4)]

$$e^{-iH_{\text{env}} t} = e^{-i\lambda t} e^{-iH_{\text{env}} t} \exp_+ \left[ -i \int_0^t d\tau \hat{F}^{\text{env}}(\tau) \right], \quad (\text{B2})$$

we obtain

$$\langle \hat{\mu}_T(t) \hat{\mu}_T(0) \rangle = e^{-i(\Delta + \lambda)t} e^{-g(t)}, \quad (\text{B3})$$

where

$$e^{-g(t)} \equiv \left\langle \hat{D}'(t) \exp_+ \left[ -i \int_0^t d\tau \hat{F}^{\text{env}}(\tau) \right] \hat{D}'(0) \right\rangle, \quad (\text{B4})$$

with

$$\hat{D}'(t) \equiv \mu_{\text{ex}} + \nu_{\text{vib}} \hat{F}_1^{\text{env}}(t). \quad (\text{B5})$$

To proceed, we introduce the generating function

$$\begin{aligned} G(t; t', t'') &\equiv \left\langle \exp_+ \left[ -i \int_t^{t''} d\tau \hat{F}_1^{\text{env}}(\tau) \right] \right. \\ &\quad \times \exp_+ \left[ -i \int_0^t d\tau \hat{F}^{\text{env}}(\tau) \right] \\ &\quad \left. \times \exp_+ \left[ -i \int_{t'}^0 d\tau \hat{F}_1^{\text{env}}(\tau) \right] \right\rangle. \end{aligned} \quad (\text{B6})$$

Equation (B4) can be evaluated via

$$e^{-g(t)} = \lim_{\substack{t'' \rightarrow t \\ t' \rightarrow 0}} (\mu_{\text{ex}} + i\nu_{\text{vib}} \partial_{t'}) (\mu_{\text{ex}} - i\nu_{\text{vib}} \partial_{t'}) G(t; t', t''). \quad (\text{B7})$$

On the other hand, the Gauss–Wick’s theorem leads to Eq. (B6) the expression

$$G(t; t', t'') = e^{-g_0(t)} e^{-g'(t; t', t'')}, \quad (\text{B8})$$

with

$$g_0(t) = \int_0^t d\tau \int_0^\tau d\tau' \langle \hat{F}^{\text{env}}(\tau) \hat{F}^{\text{env}}(\tau') \rangle, \quad (\text{B9})$$

and

$$\begin{aligned} g'(t; t', t'') &= \int_t^{t''} d\tau \int_t^\tau d\tau' \langle \hat{F}_1^{\text{env}}(\tau) \hat{F}_1^{\text{env}}(\tau') \rangle \\ &+ \int_t^{t''} d\tau \int_0^t d\tau' \langle \hat{F}_1^{\text{env}}(\tau) \hat{F}^{\text{env}}(\tau') \rangle \\ &+ \int_t^{t''} d\tau \int_{t'}^0 d\tau' \langle \hat{F}_1^{\text{env}}(\tau) \hat{F}_1^{\text{env}}(\tau') \rangle \\ &+ \int_0^t d\tau \int_{t'}^0 d\tau' \langle \hat{F}^{\text{env}}(\tau) \hat{F}_1^{\text{env}}(\tau') \rangle \\ &+ \int_{t'}^0 d\tau \int_{t'}^\tau d\tau' \langle \hat{F}_1^{\text{env}}(\tau) \hat{F}_1^{\text{env}}(\tau') \rangle. \end{aligned} \quad (\text{B10})$$

Evidently, only the middle three terms make contributions to Eq. (B7). We obtain

$$e^{-g(t)} = \left[ \left( \mu_{\text{ex}} - i\nu_{\text{vib}} \int_0^t d\tau \langle \hat{F}_1^{\text{env}}(\tau) \hat{F}_1^{\text{env}}(0) \rangle \right) \times \left( \mu_{\text{ex}} - i\nu_{\text{vib}} \int_0^t d\tau \langle \hat{F}_1^{\text{env}}(\tau) \hat{F}_1^{\text{env}}(0) \rangle \right) + \nu_{\text{vib}}^2 \langle \hat{F}_1^{\text{env}}(t) \hat{F}_1^{\text{env}}(0) \rangle \right] e^{-g_0(t)}. \quad (\text{B11})$$

Equation (63) is then resulted by substituting Eq. (B11) into Eq. (B3) together with Eq. (B9).

### Appendix C: Gas-phase limit

This appendix considers the gas-phase limit in the absence of solvent. As the limiting result of Eqs. (56) with (63), the spectrum can be derived readily and will be given in the latter half of this appendix. For just the case of gas phase, the frequency domain Fermi's golden rule will be more convenient. That is

$$S_A(\omega) = \pi \sum_{m=0}^{\infty} \sum_{n=0}^{\infty} P_n |\langle \psi'_m | \mu_{10}(\hat{q}) | \psi_n \rangle|^2 \delta(\omega - \omega_{mn}), \quad (\text{C1})$$

with  $\omega_{mn} \equiv \Delta + (m-n)\Omega$  being the transition frequency. Involved are the vibronic states,  $|\psi_n\rangle$  and  $|\psi'_m\rangle$ , from  $H_{\text{env}} = \frac{1}{2}\Omega(\hat{p}^2 + \hat{q}^2)$  and  $H'_{\text{env}} = \frac{1}{2}\Omega[\hat{p}^2 + (\hat{q} - D)^2]$ , respectively. The initial equilibrium population of  $|n\rangle$  is

$$P_n = (1 - e^{-\beta\Omega}) e^{-n\beta\Omega}. \quad (\text{C2})$$

The electronic transition dipole moment remains an operator in nuclear subspace, and is given by

$$\mu_{10}(\hat{q}) \equiv \langle 1 | \hat{\mu}_{\text{T}} | 0 \rangle = \mu_{\text{ex}} + \nu_{\text{vib}} \hat{F} = \mu_{\text{ex}} - \nu_{\text{vib}} \Omega D \hat{q}, \quad (\text{C3})$$

since  $\hat{F} = \hat{F}_1 = H'_{\text{env}} - H_{\text{env}} - \lambda_0 = -\Omega D \hat{q}$  in the gas-phase limit.

The Franck-Condon factor can be obtained as follows. By exploring the displacement operator, we obtain

$$\begin{aligned} \langle \psi'_m | \mu_{10}(\hat{q}) | \psi_n \rangle &= \langle \psi_m | e^{i\hat{p}D} \mu_{10}(\hat{q}) | \psi_n \rangle \\ &= \langle \psi_m | e^{-\frac{D}{\sqrt{2}}(\hat{a}^\dagger - \hat{a})} \mu_{10}(\hat{q}) | \psi_n \rangle \\ &= e^{-\frac{D^2}{4}} (\mu_{\text{ex}} \Lambda_{mn} - \nu_{\text{vib}} \Omega \tilde{\Lambda}_{mn}) \end{aligned} \quad (\text{C4})$$

where

$$\begin{aligned} \Lambda_{mn} &= \langle \psi_m | e^{-\frac{D}{\sqrt{2}}\hat{a}^\dagger} e^{\frac{D}{\sqrt{2}}\hat{a}} | \psi_n \rangle, \\ &= \sum_{jk} \frac{(-1)^j}{j!k!} \left( \frac{D}{\sqrt{2}} \right)^{j+k} \langle \psi_m | (a^\dagger)^j \hat{a}^k | \psi_n \rangle \\ &= \sum_{jk} \frac{(-1)^j}{j!k!} \left( \frac{D}{\sqrt{2}} \right)^{j+k} \sqrt{\frac{n!m!}{(n-k)!(m-j)!}} \delta_{m-j, n-k} \\ &= \sum_{j=0}^m \frac{(-1)^j}{j!} \sqrt{\frac{m!}{n!}} \binom{n}{m-j} \left( \frac{D}{\sqrt{2}} \right)^{n-m+2j}, \\ &\equiv \sum_{j=0}^m K_{m,n,j} \left( \frac{D}{\sqrt{2}} \right)^{n-m+2j}, \end{aligned} \quad (\text{C5})$$

with the convention  $\binom{n}{l>n} = 0$ , and

$$\begin{aligned} \tilde{\Lambda}_{mn} &= D \langle \psi_m | e^{-\frac{D}{\sqrt{2}}\hat{a}^\dagger} e^{\frac{D}{\sqrt{2}}\hat{a}} \hat{q} | \psi_n \rangle, \\ &= \frac{D}{\sqrt{2}} (\sqrt{n} \Lambda_{m,n-1} + \sqrt{n+1} \Lambda_{m,n+1}). \\ &= \sqrt{n} \sum_{j=0}^m K_{m,n-1,j} \left( \frac{D}{\sqrt{2}} \right)^{n-m+2j} \\ &\quad + S \sqrt{n+1} \sum_{j=0}^m K_{m,n+1,j} \left( \frac{D}{\sqrt{2}} \right)^{n-m+2j} \\ &= \sum_{j=0}^m \tilde{K}_{m,n,j} \left( \frac{D}{\sqrt{2}} \right)^{n-m+2j}, \end{aligned} \quad (\text{C6})$$

with  $\tilde{K}_{m,n,j} \equiv \sqrt{n} K_{m,n-1,j} + S \sqrt{n+1} K_{m,n+1,j}$ . Substituting Eqs. (C5) and (C6) into Eq. (C4) and denoting

$$R_{m,n,j} \equiv \mu_{\text{ex}} K_{m,n,j} - \nu_{\text{vib}} \Omega \tilde{K}_{m,n,j}, \quad (\text{C7})$$

we have

$$\langle \psi'_m | \mu_{10}(\hat{q}) | \psi_n \rangle = e^{-\frac{S}{2}} \sum_{j=0}^m R_{m,n,j} \left( \frac{D}{\sqrt{2}} \right)^{n-m+2j}. \quad (\text{C8})$$

Substituting it into Eq. (C1) and noticing that it is real, we obtain

$$S_A(\omega) = \pi e^{-S} \sum_{m=0}^{\infty} \sum_{n=0}^{\infty} \sum_{j=0}^m \sum_{k=0}^m R_{m,n,j} R_{m,n,k} \times S^{n-m+j+k} P_n \delta(\omega - \omega_{mn}). \quad (\text{C9})$$

To finalize, we shall convert the summation index in Eq. (C9) as

$$\sum_{m=0}^{\infty} \sum_{n=0}^{\infty} = \sum_{M=0}^{\infty} \sum_{m=M}^{\infty} + \sum_{M=-\infty}^{-1} \sum_{n=-M}^{\infty}, \quad (\text{C10})$$

by denoting  $M \equiv m - n$ . We can thus recast Eq. (C9) as

$$S_A(\omega) = \pi \sum_{M=-\infty}^{\infty} A_M \delta(\omega - \omega_M), \quad (\text{C11})$$

with  $\omega_M \equiv \omega_{mn}$  and for  $M \geq 0$

$$A_M = e^{-S} \sum_{m=M}^{\infty} P_{m-M} \sum_{j=0}^m \sum_{k=0}^m R_{m,m-M,j} \times R_{m,n-M,k} S^{j+k-M}, \quad (\text{C12a})$$

while for  $M < 0$

$$A_M = e^{-S} \sum_{n=-M}^{\infty} P_n \sum_{j=0}^{n+M} \sum_{k=0}^{n+M} R_{n+M,n,j} \times R_{n+M,n,k} S^{j+k-M}. \quad (\text{C12b})$$

Equations (C11) with (C12) and (C7) constitute the final frequency domain results on the gas-phase condition.

Particularly, in the zero-temperature limit where  $n = 0$  and  $P_0 = 1$ , we have

$$\Lambda_{m0} = \frac{(-1)^m}{\sqrt{m!}} \left( \frac{D}{\sqrt{2}} \right)^m, \quad (\text{C13a})$$

$$\tilde{\Lambda}_{m0} = \frac{(-1)^m}{\sqrt{m!}} \left( \frac{D}{\sqrt{2}} \right)^m (S - m) = (S - m) \Lambda_{m0}, \quad (\text{C13b})$$

and

$$S_A(\omega) = \pi e^{-S} \sum_{m=0}^{\infty} \frac{S^m}{m!} [\mu_{\text{ex}} - \nu_{\text{vib}} \Omega (S - m)]^2 \times \delta(\omega - \Delta - m\Omega). \quad (\text{C14})$$

Alternatively, let us recall Eqs.(56) with (63) in the gas-phase condition where  $\hat{F} = \hat{F}_1$ . We have

$$S_A(\omega) = \text{Re} \int_0^{\infty} dt e^{i(\omega - \Delta - \lambda_0)t} e^{-g(t)}, \quad (\text{C15})$$

with

$$e^{-g(t)} = \left[ \left( \mu_{\text{ex}} - i\nu_{\text{vib}} \int_0^t d\tau \langle \hat{F}_1^{\text{env}}(\tau) \hat{F}_1^{\text{env}} \rangle \right)^2 + \nu_{\text{vib}}^2 \langle \hat{F}_1^{\text{env}}(t) \hat{F}_1^{\text{env}} \rangle \right] e^{-g_0(t)}, \quad (\text{C16})$$

and

$$e^{-g_0(t)} = \exp \left[ - \int_0^t d\tau \int_0^{\tau} d\tau' \langle \hat{F}_1^{\text{env}}(\tau) \hat{F}_1^{\text{env}}(\tau') \rangle \right]. \quad (\text{C17})$$

For the gas-phase model, it is easy to obtain that

$$\langle \hat{F}_1^{\text{env}}(t) \hat{F}_1^{\text{env}} \rangle_{\text{env}} = \Omega^2 S [(\bar{n} + 1) e^{-i\Omega t} + \bar{n} e^{i\Omega t}], \quad (\text{C18})$$

with  $\bar{n} = 1/(e^{\beta\Omega} - 1)$ . Thus

$$\int_0^t d\tau \langle \hat{F}_1^{\text{env}}(\tau) \hat{F}_1^{\text{env}} \rangle_{\text{env}} = -i\Omega S [1 - (\bar{n} + 1) e^{-i\Omega t} + \bar{n} e^{i\Omega t}], \quad (\text{C19})$$

and

$$\int_0^t d\tau \int_0^{\tau} d\tau' \langle \hat{F}_1^{\text{env}}(\tau') \hat{F}_1^{\text{env}} \rangle_{\text{env}} = -i\Omega S t + S(2\bar{n} + 1) - S[(\bar{n} + 1) e^{-i\Omega t} + \bar{n} e^{i\Omega t}]. \quad (\text{C20})$$

Equation (C17) thus results in (noting that  $\lambda_0 = \Omega S$ )

$$e^{-g_0(t)} = e^{i\lambda_0 t} W(t), \quad (\text{C21})$$

with

$$\begin{aligned} W(t) &\equiv e^{-S(2\bar{n}+1)} e^{S[(\bar{n}+1)e^{-i\Omega t} + \bar{n}e^{i\Omega t}]} \\ &= \sum_{m=0}^{\infty} \sum_{n=0}^{\infty} e^{-S(2\bar{n}+1)} \frac{S^{m+n} (\bar{n}+1)^m \bar{n}^n}{m!n!} e^{-i(m-n)\Omega t} \\ &\equiv \sum_{m=0}^{\infty} \sum_{n=0}^{\infty} W_{mn} e^{-i(m-n)\Omega t}. \end{aligned} \quad (\text{C22})$$

Together with Eqs.(C18) and (C19), we obtain from Eqs.(C15) and (C16) that

$$S_A(\omega) = \pi \sum_{m=0}^{\infty} \sum_{n=0}^{\infty} \sum_{k=-2}^2 W_{mn} Y_k \delta(\omega - \omega_{mn} - k\Omega), \quad (\text{C23})$$

with

$$Y_2 = [\nu_{\text{vib}} \Omega S (\bar{n} + 1)]^2, \quad (\text{C24a})$$

$$Y_1 = [2\mu_{\text{ex}} + (1 - 2S)\nu_{\text{vib}}\Omega] \nu_{\text{vib}} \Omega S (\bar{n} + 1), \quad (\text{C24b})$$

$$Y_0 = (\mu_{\text{ex}} - \nu_{\text{vib}} \Omega S)^2 - 2\nu_{\text{vib}}^2 \Omega^2 S^2 \bar{n} (\bar{n} + 1), \quad (\text{C24c})$$

$$Y_{-1} = [-2\mu_{\text{ex}} + (1 + 2S)\nu_{\text{vib}}\Omega] \nu_{\text{vib}} \Omega S \bar{n}, \quad (\text{C24d})$$

$$Y_{-2} = (\nu_{\text{vib}} \Omega S \bar{n})^2. \quad (\text{C24e})$$

After some rearrangement of summation indices, Eq.(C23) can be recast in the form of

$$S_A(\omega) = \pi \sum_{M=-\infty}^{\infty} A'_M \delta(\omega - \omega_M). \quad (\text{C25})$$

The details are a bit tedious and not given here. The equivalence between the  $A'_M$  in Eq.(C25) and  $A_M$  of Eq.(C12) has been numerically confirmed. Depicted in Fig.3 are the linear absorption lineshapes in the gas-phase condition, evaluated via Eq.(C25) or Eq.(C11), where the  $\delta$ -functions have been broadened as Lorentz functions.

We consider again the zero-temperature limit where  $\bar{n} = 0$ , leading to

$$W(t) = e^{-S} \sum_{m=0}^{\infty} \frac{S^m}{m!} e^{-im\Omega t}, \quad (\text{C26})$$

and

$$Y_2 = (\nu_{\text{vib}} \Omega S)^2, \quad (\text{C27a})$$

$$Y_1 = [2\mu_{\text{ex}} + (1 - 2S)\nu_{\text{vib}}\Omega] \nu_{\text{vib}} \Omega S, \quad (\text{C27b})$$

$$Y_0 = (\mu_{\text{ex}} - \nu_{\text{vib}} \Omega S)^2, \quad (\text{C27c})$$

$$Y_{-1} = Y_{-2} = 0. \quad (\text{C27d})$$

We can then obtain from Eq.(C23) that

$$\begin{aligned} S_A(\omega) &= \pi e^{-S} \sum_{m=0}^{\infty} \frac{S^m}{m!} \left\{ (\nu_{\text{vib}} \Omega S)^2 \delta(\omega - \Delta - (m+2)\Omega) \right. \\ &\quad + [2\mu_{\text{ex}} + (1 - 2S)\nu_{\text{vib}}\Omega] \nu_{\text{vib}} \Omega S \delta(\omega - \Delta - (m+1)\Omega) \\ &\quad \left. + (\mu_{\text{ex}} - \nu_{\text{vib}} \Omega S)^2 \delta(\omega - \Delta - m\Omega) \right\} \\ &= \pi e^{-S} \sum_{m=0}^{\infty} \frac{S^m}{m!} \left\{ m(m-1) (\nu_{\text{vib}} \Omega)^2 + (\mu_{\text{ex}} - \nu_{\text{vib}} \Omega S)^2 \right. \\ &\quad \left. + m[2\mu_{\text{ex}} + (1 - 2S)\nu_{\text{vib}}\Omega] \nu_{\text{vib}} \Omega \right\} \delta(\omega - \Delta - m\Omega) \\ &= \pi e^{-S} \sum_{m=0}^{\infty} \frac{S^m}{m!} (\mu_{\text{ex}} - \nu_{\text{vib}} \Omega S + m\nu_{\text{vib}} \Omega)^2 \delta(\omega - \Delta - m\Omega). \end{aligned} \quad (\text{C28})$$

This is equivalent to Eq.(C14).

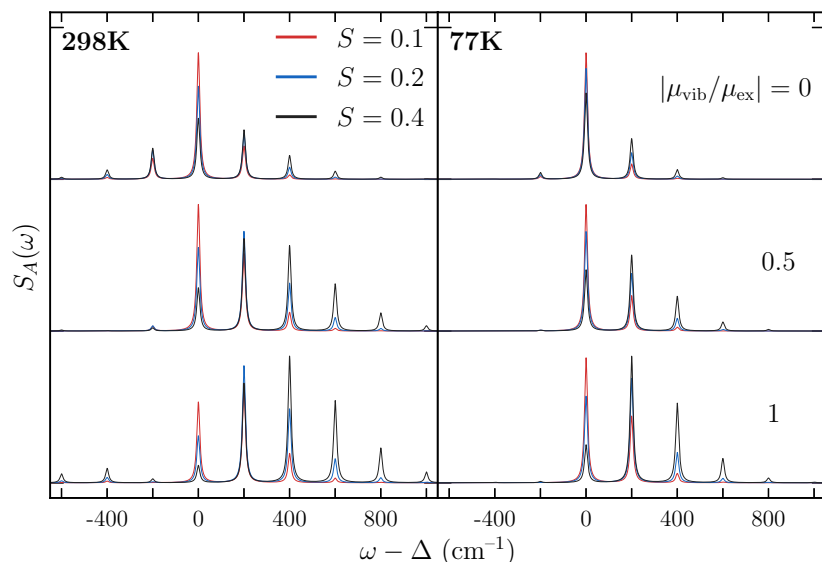


FIG. 3: Gas-phase linear absorption lineshapes at the temperatures  $T = 298\text{K}$  (left) and  $T = 77\text{K}$  (right). Other involved parameters are same as in Fig. 1.

- [1] G. D. Scholes and G. Rumbles, “Excitons in nanoscale systems,” *Nat. Mater.* **5**, 683 (2006).
- [2] N. J. Hestand and F. C. Spano, “Expanded theory of H- and J- molecular aggregates: The effects of vibronic coupling and intermolecular charge transfer,” *Chem. Rev.* **118**, 7069 (2018).
- [3] P. Forn-Díaz, L. Lamata, E. Rico, J. Kono, and E. Solano, “Ultrastrong coupling regimes of light-matter interaction,” *Rev. Mod. Phys.* **91**, 025005 (2019).
- [4] N. S. Ginsberg and W. A. Tisdale, “Spatially resolved photogenerated exciton and charge transport in emerging semiconductors,” *Annu. Rev. Phys. Chem.* **71**, 1 (2020).
- [5] T. R. Nelson, A. J. White, J. A. Bjorgaard, A. E. Sifain, Y. Zhang, B. Nebgen, S. Fernandez-Alberti, D. Mozyrsky, A. E. Roitberg, and S. Tretiak, “Non-adiabatic excited-state molecular dynamics: Theory and applications for modeling photophysics in extended molecular materials,” *Chem. Rev.* **120**, 2215 (2020).
- [6] G. S. Engel, T. R. Calhoun, E. L. Read, T. K. Ahn, T. Mančal, Y. C. Cheng, R. E. Blankenship, and G. R. Fleming, “Evidence for wavelike energy transfer through quantum coherence in photosynthetic systems,” *Nature* **446**, 782 (2007).
- [7] Y. C. Cheng and G. R. Fleming, “Dynamics of light harvesting in photosynthesis,” *Annu. Rev. Phys. Chem.* **60**, 241 (2009).
- [8] G. Panitchayangkoon, D. Hayes, K. A. Fransted, J. R. Caram, E. Harel, J. Wen, R. E. Blankenship, and G. S. Engel, “Long-lived quantum coherence in photosynthetic complexes at physiological temperature,” *Proc. Natl. Acad. Sci. USA* **107**, 12766 (2010).
- [9] M. B. Plenio, J. Almeida, and S. F. Huelga, “Origin of long-lived oscillations in 2D-spectra of a quantum vibronic model: electronic versus vibrational coherence,” *J. Chem. Phys.* **139**, 235102 (2013).
- [10] P. Kambhampati, D. H. Son, T. W. Kee, and P. F. Barbara, “Solvent effects on vibrational coherence and ultrafast reaction dynamics in the multicolor pump-probe spectroscopy of intervalence electron transfer,” *J. Phys. Chem. A* **104**, 10637 (2000).
- [11] K. Ishii, S. Takeuchi, and T. Tahara, “Pronounced non-Condon effect as the origin of the quantum beat observed in the time-resolved absorption signal from excited-state cis-stilbene,” *J. Phys. Chem. A* **112**, 2219 (2008).
- [12] J. M. Womick, B. A. West, N. F. Scherer, and A. M. Moran, “Vibronic effects in the spectroscopy and dynamics of C-phycoerythrin,” *J. Phys. B: Atomic, Molecular and Optical Physics* **45**, 154016 (2012).
- [13] D. B. Turner, K. E. Wilk, P. M. G. Curmi, and G. D. Scholes, “Comparison of electronic and vibrational coherence measured by two-dimensional electronic spectroscopy,” *J. Phys. Chem. Lett.* **2**, 1904 (2011).
- [14] R. Tempelaar, T. L. C. Jansen, and J. Knoester, “Vibrational beatings conceal evidence of electronic coherence in the FMO light-harvesting complex,” *J. Phys. Chem. B* **118**, 12865 (2014).
- [15] V. Butkus, L. Valkunas, and D. Abramavicius, “Vibronic phenomena and exciton-vibrational interference in two-dimensional spectra of molecular aggregates,” *J. Chem. Phys.* **140**, 034306 (2014).
- [16] F. V. A. Camargo, H. L. Anderson, S. R. Meech, and I. A. Heisler, “Full characterization of vibrational coherence in a porphyrin chromophore by two-dimensional electronic spectroscopy,” *J. Phys. Chem. A* **119**, 95 (2015).
- [17] V. Balevičius, A. G. Pour, J. Savolainen, C. N. Lincoln, V. Lukeš, E. Riedle, L. Valkunas, D. Abramavicius, and J. Hauer, “Vibronic energy relaxation approach highlighting deactivation pathways in carotenoids,” *Phys. Chem. Chem. Phys.* **17**, 19491 (2015).
- [18] H. D. Zhang, Q. Qiao, R. X. Xu, and Y. J. Yan, “Effects of Herzberg–Teller vibronic coupling on coherent excitation energy transfer,” *J. Chem. Phys.* **145**, 204109 (2016).
- [19] A. O. Caldeira and A. J. Leggett, “Path integral approach to quantum Brownian motion,” *Physica A* **121**, 587 (1983).

- [20] U. Weiss, *Quantum Dissipative Systems*, World Scientific, Singapore, 2012, 4<sup>th</sup> ed.
- [21] Y. J. Yan and R. X. Xu, “Quantum mechanics of dissipative systems,” *Annu. Rev. Phys. Chem.* **56**, 187 (2005).
- [22] A. G. Redfield, “The theory of relaxation processes,” *Adv. Magn. Reson.* **1**, 1 (1965).
- [23] G. Lindblad, “On the generators of quantum dynamical semigroups,” *Commun. Math. Phys.* **48**, 119 (1976).
- [24] V. Gorini, A. Kossakowski, and E. C. G. Sudarshan, “Completely positive dynamical semigroups of  $N$ -level systems,” *J. Math. Phys.* **17**, 821 (1976).
- [25] S. Hershfield, “Equivalence of the multilead approach to dephasing and the self-consistent Born approximation,” *Phys. Rev. B* **43**, 11586 (1991).
- [26] Y. J. Yan, “Quantum Fokker-Planck theory in a non-Gaussian-Markovian medium,” *Phys. Rev. A* **58**, 2721 (1998).
- [27] Y. J. Yan, F. Shuang, R. X. Xu, J. X. Cheng, X. Q. Li, C. Yang, and H. Y. Zhang, “Unified approach to the Bloch-Redfield theory and quantum Fokker-Planck equations,” *J. Chem. Phys.* **113**, 2068 (2000).
- [28] V. I. Novoderezhkin, M. A. Palacios, H. van Amerongen, and R. van Grondelle, “Energy-Transfer Dynamics in the LHCI Complex of Higher Plants: Modified Redfield Approach,” *J. Phys. Chem. B* **108**, 10363 (2004).
- [29] M. Schröder, U. Kleinekathöfer, and M. Schreiber, “Calculation of absorption spectra for light-harvesting systems using non-Markovian approaches as well as modified Redfield theory,” *J. Chem. Phys.* **124**, 084903 (2006).
- [30] Y. Tanimura and R. Kubo, “Time evolution of a quantum system in contact with a nearly Gaussian-Markovian noise bath,” *J. Phys. Soc. Jpn.* **58**, 101 (1989).
- [31] Y. A. Yan, F. Yang, Y. Liu, and J. S. Shao, “Hierarchical approach based on stochastic decoupling to dissipative systems,” *Chem. Phys. Lett.* **395**, 216 (2004).
- [32] A. Ishizaki and Y. Tanimura, “Quantum dynamics of system strongly coupled to low temperature colored noise bath: Reduced hierarchy equations approach,” *J. Phys. Soc. Jpn.* **74**, 3131 (2005).
- [33] Y. Tanimura, “Stochastic Liouville, Langevin, Fokker-Planck, and master equation approaches to quantum dissipative systems,” *J. Phys. Soc. Jpn.* **75**, 082001 (2006).
- [34] R. X. Xu, P. Cui, X. Q. Li, Y. Mo, and Y. J. Yan, “Exact quantum master equation via the calculus on path integrals,” *J. Chem. Phys.* **122**, 041103 (2005).
- [35] R. X. Xu and Y. J. Yan, “Dynamics of quantum dissipation systems interacting with bosonic canonical bath: Hierarchical equations of motion approach,” *Phys. Rev. E* **75**, 031107 (2007).
- [36] J. S. Jin, X. Zheng, and Y. J. Yan, “Exact dynamics of dissipative electronic systems and quantum transport: Hierarchical equations of motion approach,” *J. Chem. Phys.* **128**, 234703 (2008).
- [37] L. P. Chen, R. H. Zheng, Y. Y. Jing, and Q. Shi, “Simulation of the two-dimensional electronic spectra of the Fenna-Matthews-Olson complex using the hierarchical equations of motion method,” *J. Chem. Phys.* **134**, 194508 (2011).
- [38] L. Z. Ye, X. L. Wang, D. Hou, R. X. Xu, X. Zheng, and Y. J. Yan, “HEOM-QUICK: A program for accurate, efficient and universal characterization of strongly correlated quantum impurity systems,” *WIREs Comp. Mol. Sci.* **6**, 608 (2016).
- [39] Y. Tanimura, “Numerically “exact” approach to open quantum dynamics: The hierarchical equations of motion (HEOM),” *J. Chem. Phys.* **153**, 020901 (2020).
- [40] Y. J. Yan, “Theory of open quantum systems with bath of electrons and phonons and spins: Many-dissipaton density matrixes approach,” *J. Chem. Phys.* **140**, 054105 (2014).
- [41] H. D. Zhang, R. X. Xu, X. Zheng, and Y. J. Yan, “Non-perturbative spin-boson and spin-spin dynamics and nonlinear Fano interferences: A unified dissipaton theory based study,” *J. Chem. Phys.* **142**, 024112 (2015).
- [42] Y. J. Yan, J. S. Jin, R. X. Xu, and X. Zheng, “Dissipaton equation of motion approach to open quantum systems,” *Frontiers Phys.* **11**, 110306 (2016).
- [43] R. X. Xu, Y. Liu, H. D. Zhang, and Y. J. Yan, “Theories of quantum dissipation and nonlinear coupling bath descriptors,” *J. Chem. Phys.* **148**, 114103 (2018).
- [44] H. D. Zhang, R. X. Xu, X. Zheng, and Y. J. Yan, “Statistical quasi-particle theory for open quantum systems,” *Mol. Phys.* **116**, 780 (2018), Special Issue, “Molecular Physics in China”.
- [45] Y. Wang, R. X. Xu, and Y. J. Yan, “Entangled system-and-environment dynamics: Phase-space dissipaton theory,” *J. Chem. Phys.* **152**, 041102 (2020).
- [46] P. L. Du, Y. Wang, R. X. Xu, H. D. Zhang, and Y. J. Yan, “System-bath entanglement theorem with Gaussian environments,” *J. Chem. Phys.* **152**, 034102 (2020).
- [47] X. Zheng, J. Y. Luo, J. S. Jin, and Y. J. Yan, “Complex non-Markovian effect on time-dependent quantum transport,” *J. Chem. Phys.* **130**, 124508 (2009).
- [48] J. J. Ding, J. Xu, J. Hu, R. X. Xu, and Y. J. Yan, “Optimized hierarchical equations of motion for Drude dissipation with applications to linear and nonlinear optical responses,” *J. Chem. Phys.* **135**, 164107 (2011).
- [49] H. D. Zhang, Q. Qiao, R. X. Xu, X. Zheng, and Y. J. Yan, “Efficient steady-state solver for hierarchical quantum master equations,” *J. Chem. Phys.* **147**, 044105 (2017).
- [50] R. X. Xu, B. L. Tian, J. Xu, and Y. J. Yan, “Exact dynamics of driven Brownian oscillators,” *J. Chem. Phys.* **130**, 074107 (2009).